Cobalt and nickel aluminate spinels: Blue and cyan pigments

Manuel Gaudon, Lionel Robertson, Emilie Lataste, Mathieu Duttine, Michel Ménétrier, Alain Demourgues

Cobalt and nickel aluminate spinels: Blue and cyan pigments

M. Gaudon*, L.C. Robertson, E. Lataste, M. Duttine, M. Ménétrier, A. Demourgues

CNRS, University of Bordeaux, ICMCB, 87 avenue Dr Albert Schweitzer, 33600 Pessac, France

Abstract

M^{2+}-doped aluminate spinels (M=Co or Ni) were prepared by a polymeric route leading to pure phases for synthesis temperatures equal to 800 or 1200 °C and characterized by UV–vis–NIR spectroscopy, ^{27}Al NMR and XRD refinements. Coloration of the synthesized pigments is clearly sensitive to the distribution of doping ions in the aluminate spinel lattice. As the synthesis temperature increased, a color shift from green to blue has been observed for $Zn_{1-x}Co_xAl_2O_4$ compound while coloration of $Zn_{1-x}Ni_xAl_2O_4$ compound remains greenish-gray. Hence, to improve pigment coloration and/or synthesis cost, two different strategies have been proposed: (i) the synthesis of aluminum over-stoichiometric spinel with $Zn_{0.9}Co_{0.1}Al_{2.2}O_{4+\delta}$ formal composition in order to force Co^{2+} to be located in tetrahedral sites and (ii) changing from $ZnAl_2O_4$ to $MgAl_2O_4$ as host lattices for Ni^{2+} doping ions in order to force Ni^{2+} to be located in octahedral sites.

1. Introduction

Synthetic blue pigments are widely used in the ceramics industry as coloring agents for glazes or porcelain stoneware [1–2]. The traditional source of blue color in a ceramic pigment remains the divalent cobalt ion (Co^{2+}) in tetrahedral coordination site [3], especially inside the $CoAl_2O_4$ spinel phase [1–16]. However, recent publications have focused on the elaboration of aluminate spinels for cyan pigments (one primary color in subtractive system) with Ni^{2+} as chromophore ion [17–19].

The main drawback of $CoAl_2O_4$ blue pigment lies in the large range of colorimetric parameters depending on material thermal history. Indeed, the $CoAl_2O_4$ composition (known as Thenard's blue) is known for exhibiting a sky-blue hue more intense after high temperature treatment [6–12] than after moderate annealing. Previous literature work [6–10,20–22] and more especially our own previous study [16] on $Zn_{1-x}Co_xAl_2O_4$ oxides have underlined the influence of thermal history on the pigment coloration and reported this "becoming-green" phenomenon with decreasing synthesis temperature. Presently, a clear consensus [16,20–24] shows that the effect is due to the variation of the distribution of the cobalt cations between octahedral and tetrahedral sites of the spinel network, with the possibility to obtain a pink ceramic as an extreme effect when Co^{2+} ions are entirely located in octahedral site [21].

In this study, $Zn_{0.9}Co_{0.1}Al_2O_4$ powder was elaborated by a Pechini route [25] and thereafter annealed at various temperatures between 800 and 1200 °C. Combined analysis of diffuse reflectance spectra, X-Ray diffraction patterns and ^{27}Al NMR spectra clearly shows that the green color of pigments issued from low temperature treatments is due to cationic and anionic deficient spinels with tetrahedral vacancies accompanied by a partial fraction of Co^{2+} in octahedral sites as shown in our previous study [16]. In this paper, it is shown that the solution to this "problem", considering that high thermal treatments increase the production cost significantly, is to synthesize aluminum over-stoichiometric spinel with $Zn_{0.9}Co_{0.1}Al_{2+d}O_4$ formulation.

Another study is devoted to the preparation $Zn_{0.9}Ni_{0.1}Al_2O_4$ compounds by the same Pechini route as previously, with thermal treatments varying between 800 and 1200 °C. As for the zinc–cobalt aluminates, color evolution is observed with the zinc–nickel pigments thermal history. Furthermore, poor colorations besides pigment application: greenish grays, are only obtained and linked to the cationic distribution of the

*Corresponding author. Tel.: +33 5400 066 85; fax: +33 5400 027 61.
E-mail address: gaudon@icmcb-bordeaux.cnrs.fr (M. Gaudon).

Ni^{2+} chromophore ions in the spinel framework. In a parallel way to the case of zinc–cobalt aluminates, a strategy was found in order to synthesize beautiful cyan pigments with coloration arising from the occurrence of Ni^{2+} ions only in octahedral sites: synthesizing $Mg_{0.9}Ni_{0.1}Al_2O_4$ spinel compounds instead of the $Zn_{0.9}Ni_{0.1}Al_2O_4$ compounds.

2. Experimental

The nickel and cobalt pigments were synthesized by the Pechini route [25]. This chemical process is based on cations chelation by citric acid (CA) and on polyesterification between CA and ethylene glycol (EG) which leads to the formation of a polycationic resin. Aqueous solutions of citrate were prepared by dissolving CA in a minimal volume of water. Then, cationic salts: $ZnCl_2$, $Co(NO_3)_2 \cdot 6H_2O$ and $Al(NO_3)_3 \cdot 6H_2O$ were added in stoichiometric proportion to the acid solution. CA/cations molar ratio equal to 3/1 was used. After complete dissolution of the metallic salts, EG was added with a 4/1 EG/CA molar ratio. EG–CA polymerization was promoted by removing water with continuous heating on a hot plate. Then, the highly viscous mixtures were thermally treated in two steps: a first calcination at 300 °C for 10 h, then, an annealing step for 20 h between 800 °C and 1200 °C; the annealing and cooling rates were fixed to 2 °C min^{-1} while it is known that cooling rate can slightly the cationic distribution inside spinel compounds [26].

X-Ray diffraction (XRD) measurements were carried out on a PANalytical X'PERT PRO diffractometer equipped with a X-celerator detector, using Cu($K\alpha_1/K\alpha_2$) radiation. Diffractograms have been analyzed by Rietveld refinement method using FULLPROF® program package [27]. Unit cell parameters, atomic positions and occupancies as well as the Debye Weller factors (isotropic displacement factors) were refined in space group *Fd-3m* corresponding to the spinel structure.

^{27}Al MAS (spin rate 30 kHz) NMR spectra were recorded with a Bruker 500 solid state spectrometer at 130.3 MHz. A single pulse sequence was used with a 1 μs pulse width (corresponding to a $\pi/12$ flip angle for a liquid sample) and a 30 s recycle delay. The 0 ppm reference was set to a 1 M aluminum nitrate solution using the secondary solid state reference $Al(PO_3)_3$ (−21.4 ppm).

Diffuse absorption spectra were recorded at room temperature from 200 to 800 nm (1 nm step; 2 nm band length) with a Cary 17 spectrophotometer using an integration sphere. Halon was used as white reference. Mathematic treatment of the obtained spectra allowed the determination of colorimetric parameters in RGB space. The first step consists in obtaining XYZ tri-stimulus values (defined by the CIE, 1964) from integration (on the visible range, i.e. from $\lambda = 380$ nm up to 780 nm) of the product of $x(\lambda)$, $y(\lambda)$ or $z(\lambda)$ functions (CIE-1964) with the diffuse reflectance spectra function: $X = \int x(\lambda) R(\lambda) d\lambda$. Thereafter, the transfer equations defined by the CIE, 1976, from XYZ space to the RGB space, were used in order to obtain RGB chromatic parameters. RGB is used herein (instead of the commonly used $L^*a^*b^*$ chromatic parameters) in order to allow everyone to simulate the corresponding coloration with common drawing software.

3. Results and discussion

3.1. $Zn_{0.9}(Ni_{0.1}/Co_{0.1})Al_2O_4$ pigments

Reflectance spectra were recorded in the near-UV/visible/near-IR range for $Zn_{0.9}Co_{0.1}Al_2O_4$ compounds prepared at 800 °C and 1200 °C (Fig. 1). The d–d bands appearing at about 600 nm are well known to be relative to the Co^{2+} ion in tetrahedral coordination: these bands were indexed as $^4A_2 \rightarrow {}^4T_1$ transition, which can be decomposed as a triplet due to the L-S Russel–Saunders coupling. The intensity of this triplet drastically increases with annealing temperature between 800 °C and 1200 °C. This phenomenon already reported in literature [16,21,23] is related to the increase of cobalt fraction in tetrahedral site. A series of convoluted gaps with ligand oxygen-to-metal cations (Co^{2+} or Zn^{2+}) charge transfers can be observed near the UV–vis frontier. A blue coloration adequate for pigment applications can thus be achieved for this chemical composition only when high annealing temperature is performed (1200 °C).

For $Zn_{0.9}Ni_{0.1}Al_2O_4$ compounds prepared at 800 °C and 1200 °C, reflectance spectra recorded in the near-UV/visible/near-IR range (Fig. 2) exhibit intense convoluted bands in UV–vis range due to oxygen to Ni^{2+} and Zn^{2+} charge transfers, and a doublet at about 600 and 630 nm. These d–d bands, as a doublet, can be attributed to Ni^{2+} in octahedral field according to literature on nickelate spinels [17–19]. Nevertheless, this attribution remains subjective and open to criticism without more detailed investigations in the infrared range. However, the low intensity of these d–d bands is consistent with an attribution to centro-symmetric sites. Actually, the colors which are reached, are unsaturated (greenish gray) and not adequate for pigments applications.

Rietveld refinements of X-ray diffraction patterns were performed for cobalt and nickel-doped compounds obtained after annealing at 800 °C and 1200 °C. A graphical illustration of experimental, calculated and difference signals is reported in Fig. 3, for the nickel-doped samples. Obviously the peak width decreases as annealing temperature increases, revealing an increase in crystallite size. Crystallite size can be roughly

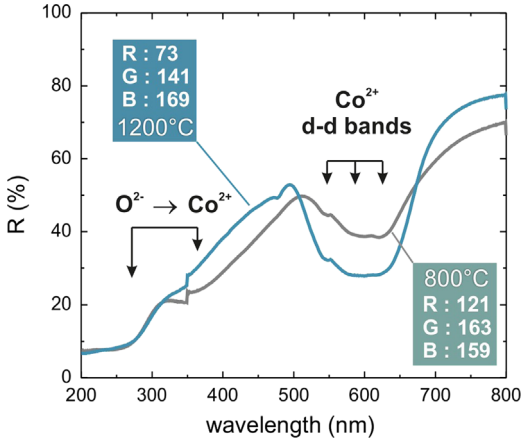

Fig. 1. Diffuse reflectance spectra ($R\%$) of $Zn_{0.9}Co_{0.1}Al_2O_4$ compound prepared at 800 °C and 1200 °C.

estimated from the full width at half-maximum of diffraction peaks, using the Debye–Scherer equation. For $Zn_{0.9}Co_{0.1}Al_2O_4$ sample the crystallite size is estimated about 30 nm and 110 nm after annealing at respectively 800 °C and 1200 °C; for $Zn_{0.9}Ni_{0.1}Al_2O_4$ sample the size is estimated at 20 nm after annealing at 800 °C and 80 nm after 1200 °C annealing. Smaller crystallite sizes were obtained for the Ni^{2+}-doped compounds. Due to their electronic configuration similarity to Al^{3+} ions, Zn^{2+}, Co^{2+} and Ni^{2+} cations can barely be distinguished by XRD Rietveld refinements thus, only Zn^{2+} was considered as A^{2+} ion. Furthermore, refinements were performed considering no atomic vacancy, i.e. with only inversion rate as occupancy parameter. Refined parameters and reliability factors are reported in Table 1. The inversion rate of $Zn_{0.9}Co_{0.1}Al_2O_4$ slightly decreased with annealing temperatures: from 12 to 7% at respectively, 800 °C and 1200 °C; whereas, opposite behavior was observed for $Zn_{0.9}Ni_{0.1}Al_2O_4$, with a moderate increase of inversion rate from 10 to 12% between 800 °C and 1200 °C. According to ^{27}Al NMR analysis of non-doped $ZnAl_2O_4$ annealed at 800 and 1200 °C, the un-doped matrix can be considered as an almost direct spinel. NMR spectra (Fig. 4) both show an intense peak at about 10 ppm which is characteristic of six-fold coordination for Al^{3+} ions and, at 70 ppm, with a very weak and narrow signal attributed to four-fold coordinated Al^{3+} [16,28–29]. Thus the global inversion rate obtained from X-ray diffractogram refinements (Table 1) appears to be essentially related (representative) to the Co^{2+} or Ni^{2+} distribution which is consistent with the evolution of d–d bands (associated with either Co^{2+} ions in tetrahedral sites or Ni^{2+} ions in octahedral environment) intensity observed in reflectance spectra. Unfortunately, even after high temperature annealing, a small part of Co^{2+} located in octahedral sites or Ni^{2+} in tetrahedral sites depending of the composition, pollute the compound color and limit their application as pigment.

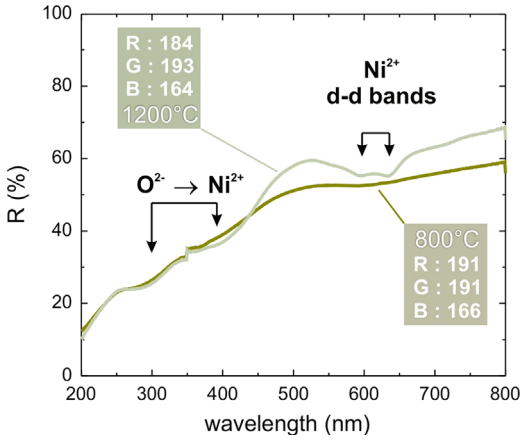

Fig. 2. Diffuse reflectance spectra (*R*%) of $Zn_{0.9}Ni_{0.1}Al_2O_4$ compound prepared at 800 °C and 1200 °C.

3.2. $Zn_{0.9}Co_{0.1}Al_{2.2}O_{4+d}$ pigment

In order to improve the pigment quality of the co-doped zinc aluminates, our idea was to synthesize Al-over-stoichiometric compound with formulae: $Zn_{0.9}Co_{0.1}Al_{2.2}O_{4+d}$. Indeed, the over-stoichiometry of six-fold coordinated cation, i.e. the over-saturation of the octahedral sub-network with Al^{3+} ions, could tend to stabilize a higher fraction of Co^{2+} only in tetrahedral coordination. It can be noticed that the presentation of this

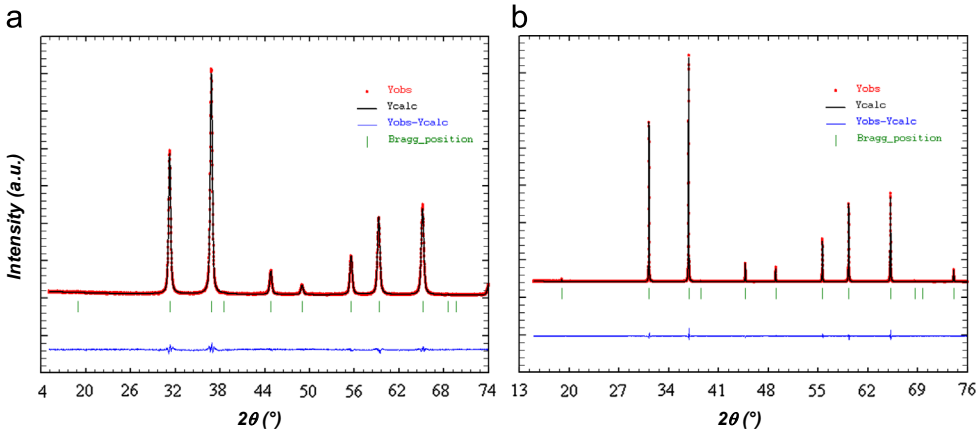

Fig. 3. Rietveld refinement of XRD patterns (experimental. calculated and difference) of $Zn_{0.9}Ni_{0.1}Al_2O_4$ annealed at 800 °C (a) and 1200 °C (b).

Table 1
Cell parameter, oxygen atomic position, B_{iso} displacements, γ inversion rate and reliability factors for various spinel phases.

Composition	Annealing ***T*** °C	**a (Å)**	**32e** Position	B_{iso} (per site) (Å^2)	**Al inv. rate**	**Reliabilty factor**
$Zn_{0.9}Co_{0.1}Al_2O_4$	800	**8.0882**	**0.2628**	0.47 (8a) 0.36 (16d) 0.67 (32e)	**12%**	C_{Rp}=9%C_{Rwp}=9%R_{bragg}=**2.01**
	1200	**8.0895**	**0.2639**	0.26 (8a) 0.22 (16d) 0.34 (32e)	**7%**	C_{Rp}=8%C_{Rwp}=9%R_{bragg}=**1.95**
$Zn_{0.9}Ni_{0.1}Al_2O_4$	800	**8.0895**	**0.2634**	0.47 (8a) 0.46 (16d) 0.44 (32e)	**10%**	C_{Rp}=6%C_{Rwp}=8%R_{bragg}=**1.56**
	1200	**8.0887**	**0.2633**	0.22 (8a) 0.32 (16d) 0.30 (32e)	**12%**	C_{Rp}=5%C_{Rwp}=7%R_{bragg}=**1.10**
$Mg_{0.9}Ni_{0.1}Al_2O_4$	1200	**8.0806**	**0.2590**	0.78 (8a) 0.45 (16d) 0.74 (32e)	**12%**	C_{Rp}=6%C_{Rwp}=8%R_{bragg}=**2.09**

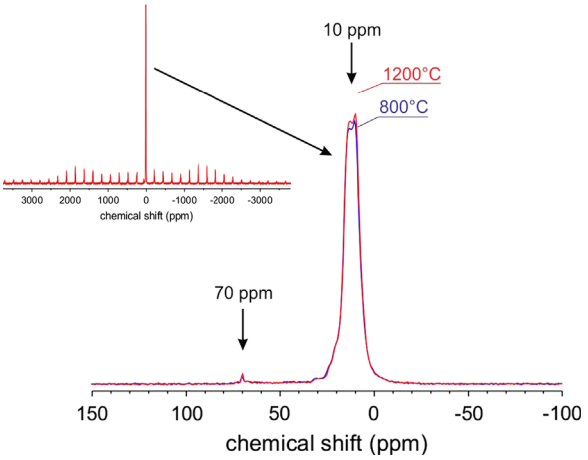

Fig. 4. ^{27}Al MAS NMR spectra of $ZnAl_2O_4$ samples annealed at 800 °C or 1200 °C. The whole set of spinning sidebands of the spectrum is shown with an expansion of the isotropic signals.

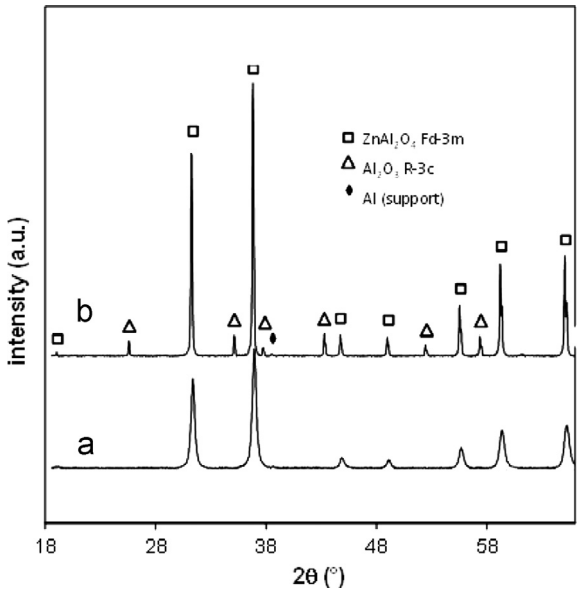

Fig. 5. X-ray diffraction patterns of $Zn_{0.9}Co_{0.1}Al_{2.2}O_4$ compounds annealed at 800 °C (a) and 1200 °C (b).

phase with a content of oxygen over 4.0 is obviously not describing the crystal framework stoichiometry since no interstitial anionic positions are offered by the spinel compounds; a more academic but complex chemical composition for our compound can be written: $Zn_{0.84}Co_{0.09}Al_{2.04}O_4$ (this last composition described better the lack of tetrahedral ions besides the excess of aluminum ions). In Fig. 5, XRD pattern of the 800 °C annealed compound shows the presence of a single crystalline phase corresponding to the spinel with crystallite size estimated to 12 nm only. Thus, even if the over-stoichiometry of Al delayed the initiation of the crystallization, a pure over-stoichiometric spinel was obtained by Pechini route at relatively low temperature. On the contrary, X-ray diffraction analysis of the compound annealed at 1200 °C shows the presence of a second phase, Al_2O_3, in addition to the spinel main phase, revealing the occurrence of a phase separation process due to the "metastable" character of over-stoichiometric spinel. Nevertheless, from a colorimetric point of view the latter experiment was a great success considering the brighter and more intense blue colorations obtained for these over-stoichiometric phases. Reflectance spectra recorded in the near-UV/visible/near-IR range are reported in Fig. 6 for the $Zn_{0.9}Co_{0.1}Al_{2.2}O_4$ compounds prepared at 800 °C and 1200 °C. The $^4A_2 \rightarrow {}^4T_1$ triple transition characteristic of the four-fold coordinated Co^{2+} ions was drastically increased compared to stoichiometric compounds and undoubtedly confirmed the presence of Co^{2+} ions in tetrahedral sites. After background subtraction and Kubelka–Munk transform, the signal is fitted by the convolution of three main Gaussian components characterized by $K/S_i = I/\exp[(E-E_0)^2/k]$ and a full width at half-maximum equal tofwhm $= 2\sqrt{k\ln(2)}$ (Fig. 7). The characteristic values of these bands are summarized in Table 2. The three maxima positions at respectively 1.63, 1.80 and 1.94 eV are in perfect agreement with the $^4A_2 \rightarrow {}^4T_1$ triple transition attributed to Co^{2+} in $Zn_{1-x}Co_xAl_2O_4$ compound, as previously reported [16]. The obvious increase of K/S intensities with annealing temperatures shows that despite the α-Al_2O_3 phase separation, the spinel phase exhibits a more and more normal cationic distribution.

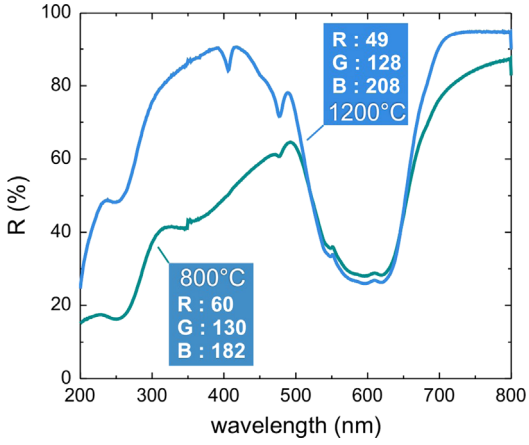

Fig. 6. Diffuse reflectance spectra ($R\%$) of $Zn_{0.9}Co_{0.1}Al_{2.2}O_4$ compound prepared at 800 °C (a) and 1200 °C (b).

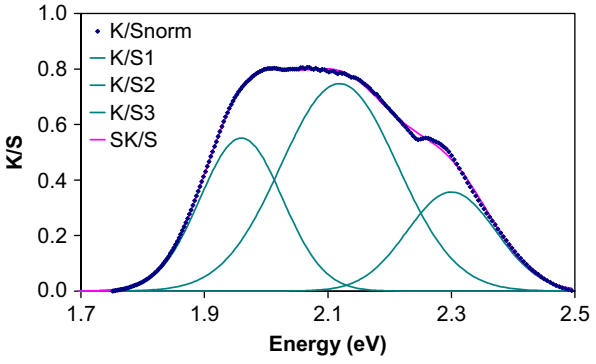

Fig. 7. K/S spectra of the d–d triplet of Co^{2+} ion for $Zn_{0.9}Co_{0.1}Al_{2.2}O_4$ compound annealed at 1200 °C and its deconvolution.

Table 2
Co^{2+} d–d bands parameters obtained from the deconvolution of $Zn_{0.9}Co_{0.1}Al_{2.2}O_{4+d}$ *K/S* spectrum (Fig. 7).

Paramètres	1200 °C Annealing			800 °C Annealing		
	K/S_1	K/S_2	K/S_3	K/S_1	K/S_2	K/S_3
E_0 (eV)	1.966	2.126	2.309	1.928	2.087	2.270
I (u.a.)	0.551	0.747	0.357	0.211	0.286	0.137
k	0.009	0.018	0.010	0.007	0.015	0.009
χ^2	1.753			2.680		

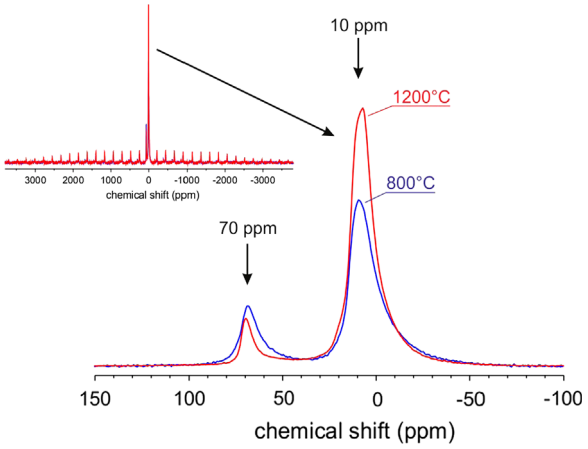

Fig. 8. ^{27}Al MAS NMR spectra of $MgAl_2O_4$ samples annealed at 800 °C or 1200 °C. The whole set of spinning sidebands of the spectrum is shown with an expansion of the isotropic signals.

3.3. $Mg_{0.9}Ni_{0.1}Al_2O_4$ pigment

According to previous results and literature, a way to improve the color saturation of Ni-doped zinc aluminates might be to force Ni^{2+} ions to occupy tetrahedral sites in the spinel lattice. With that in mind, we tried to synthesize Ni-doped zinc over-stoichiometric spinel following the same line of reasoning that we presented above for Co-doped zinc aluminates. Unfortunately, the synthesis produced the ZnO phase in addition to the spinel main phase even with annealing at low temperature. Furthermore, the colors obtained are very poorly saturated and difficult to interpret (maybe because of the presence in significant amount of nickel ions inside the würtzite phase). Another attempt consisted to replace the $ZnAl_2O_4$ host matrix by the $MgAl_2O_4$ one which is known to exhibit higher inversion rates. ^{27}Al NMR spectra of the $MgAl_2O_4$ spinel phase (Fig. 8) show indeed a four-fold coordinated Al signal (δ_{iso} = 70 ppm) clearly more intense than for $ZnAl_2O_4$ phases (Fig. 4); the observation being in good agreement with literature [30–31]. Moreover, the intensity ratio of the 70 ppm peak over the 10 ppm peak (six-fold coordinated Al) decreased with increasing annealing temperature. Fig. 9 shows X-ray diffraction patterns of the phases obtained after calcinations at 800 °C and 1200 °C. At 800 °C the synthesis produced a nano-sized spinel (crystallite size about 8 nm) and at 1200 °C, a well-crystallized phase with crystallite of ~45 nm in size. These results show the delay of the germination-growth process at high temperatures for this composition in comparison to the zinc aluminates spinels. Unfortunately, the low crystalline degree of the phase obtained at 800 °C does not allow refining the X-ray pattern using the Rietveld method. Thus, only XRD pattern of the 1200 °C annealed sample was refined (Fig. 10); the main calculated parameters are reported in Table 1. At this point, it has to be underlined that for such compositions, the specific inversion rate of Ni^{2+} ions can be estimated because Mg^{2+} and Al^{3+} electron number are similar to each other but quite different from those of Ni^{2+}. The refinements can then be performed considering the same diffusive factors for Al^{3+} and Mg^{2+} ions. Analysis of XRD pattern indicates that all nickel ions are in octahedral sites.

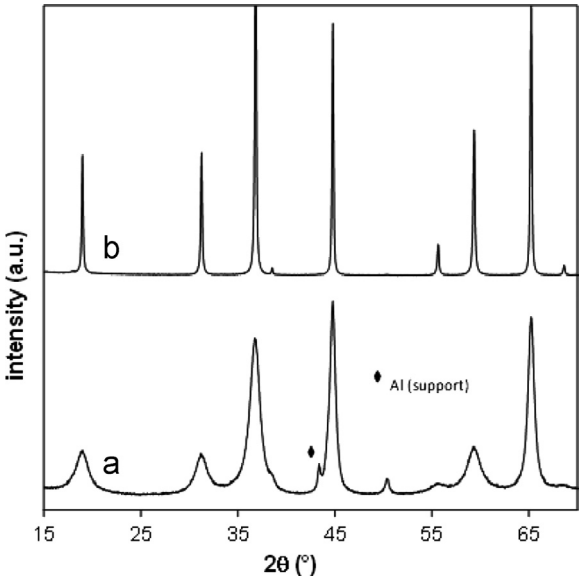

Fig. 9. X-ray diffraction patterns of $Mg_{0.9}Ni_{0.1}Al_2O_4$ compounds annealed at 800 °C (a) and 1200 °C (b).

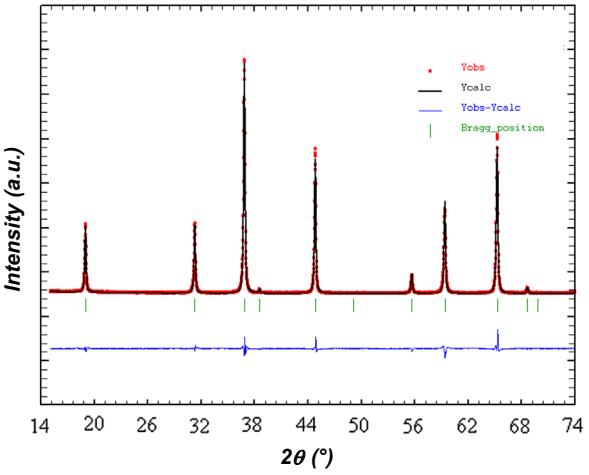

Fig. 10. Rietveld refinement spectra (experimental, calculated and difference) of $Mg_{0.9}Ni_{0.1}Al_2O_4$ composition annealed at 1200 °C.

Reflectance spectra of $Mg_{0.9}NiO_{0.1}Al_2O_4$ compounds prepared at 800 °C and 1200 °C recorded in the near-UV/visible/near-IR range are reported in. The d–d transitions at about 2 eV (600–650 nm) are more intense than for $Zn_{0.9}NiO_{0.1}Al_2O_4$ compounds and consequently, the coloration is more saturated, an interesting cyan coloration being obtained for the 1200 °C compound. Furthermore, a d–d band at about 400 nm is also observed in both spectra. These two sets of bands clearly indicate the presence of Ni^{2+} in octahedral sites. The 400 nm band can be attributed, basing on Tanabe–Sugano diagrams, to the $^3A_2 \rightarrow {}^3T(F)$ transition and the 600–650 nm multiplet to the $^3A_2 \rightarrow {}^3T_1(F)$ transition [17,32–33]. The presence of a multiplet for the latter transition was already observed in literature for $Mg_{1-x}Ni_xAl_2O_4$ spinel compounds and interpreted as an effect of the Jahn–Teller distortion of octahedral site [17,34]. After background subtraction and Kubelka–Munk transform, the signals observed in visible region were fitted using five Gaussian components (Fig. 11) whose parameters are reported in Table 3. The results show that the main triplet at 1.95, 2.08, 2.24 eV attributed to Ni^{2+} in octahedral field increases significantly with annealing temperature while two other small contributions (even if the assignment to a doublet band can be contested, since the signal in the visible region appears convoluted) at 1.64 and 1.79 eV tend on the contrary to disappear and are consistently attributed to Ni^{2+} associated to a tetrahedral field ($^3T_1 \rightarrow {}^3T_1(P)$ transition could correspond).

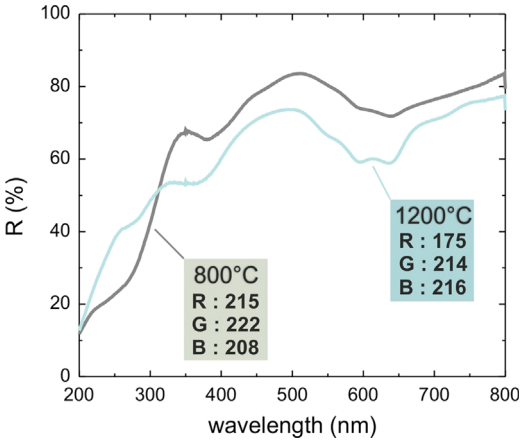

Fig. 11. Diffuse reflectance spectra (*R%*) of $Mg_{0.9}Ni_{0.1}Al_{2.2}O_4$ compound prepared at 800 °C and 1200 °C.

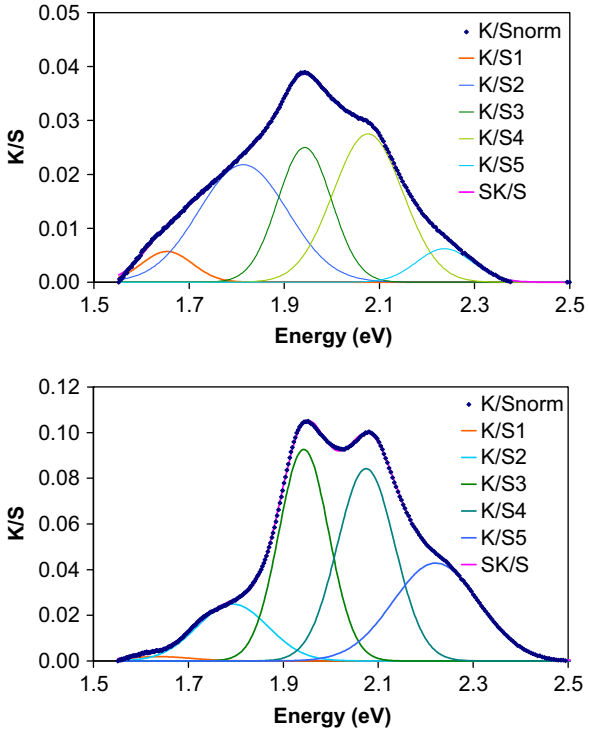

Fig. 12. *K/S* spectra of the d–d multiplet bands of Ni^{2+} ion for $Mg_{0.9}Ni_{0.1}Al_2O_4$ compound annealed at 1200 °C and its deconvolution.

Hence, with a paradoxical manner, that $MgAl_2O_4$ exhibits higher inversion rates than $ZnAl_2O_4$, the content of doping Ni^{2+} ions in octahedral sites is higher (total) for the magnesium aluminates than for the zinc aluminates. It can be proposed that the introduction of some Mg^{2+} ions inside the octahedral sites leads to a distortion and thus a "acclimation" of the cationic sub-network formed by the close packing of the octahedral sites (edge-sharing octahedral sites formed quite dense plans). The consequence is the easiest incorporation of Ni^{2+} ions in an "already" high inversion rate spinel.

4. Conclusion

$Zn_{1-x}Co_xAl_2O_4$ and $Zn_{1-x}Ni_xAl_2O_4$ compounds exhibit a coloration strongly influenced by the sample thermal history due to the influence on the synthesis temperature on the M^{2+} (Co^{2+}/Ni^{2+}) distribution between the octahedral and tetrahedral sites of the spinel network. The occurrence of a non-negligible fraction of Co^{2+} ions in octahedral sites and, in a reverse way, the occurrence of a non-negligible part of Ni^{2+} ions in tetrahedral sites act to the detriment of the pigment hue and saturation. The synthesis of aluminum over-stoichiometric spinel with $Zn_{0.9}Co_{0.1}Al_{2.2}O_{4+\delta}$ formal composition at low

Table 3
Ni^{2+} d–d bands parameters obtained from the deconvolution of $Mg_{0.9}Ni_{0.1}Al_2O_4$. *K/S* spectrum (Fig. 12).

Parameters	1200 °C annealing					800 °C annealing				
	K/S_1	K/S_2	K/S_3	K/S_4	K/S_5	K/S_1	K/S_2	K/S_3	K/S_4	K/S_5
E_0 (eV)	1.636	1.793	1.943	2.075	2.221	1.656	1.816	1.946	2.080	2.241
I (u.a.)	0.002	0.025	0.093	0.084	0.043	0.006	0.022	0.025	0.028	0.006
k	0.010	0.011	0.006	0.007	0.016	0.006	0.018	0.006	0.011	0.007
χ^2	0.016					0.032				

temperature to prevent Al_2O_3 phase separation (and to diminish the synthesis cost), helped obtaining bright blue pigments. Indeed, the relative excess of Al^{3+} in the cationic sub-network in comparison with Co^{2+} and Zn^{2+} prevents the occurrence of these A^{2+} ions location in the octahedral sites, even after synthesis at low temperatures. Basing on similar reasoning, the use of $MgAl_2O_4$ instead of $ZnAl_2O_4$ as host lattice for Ni^{2+} doping, leads to the complete stabilization of Ni^{2+} ions in octahedral sites. Thus, $Mg_{0.9}Ni_{0.1}Al_2O_4$ composition sintered at 1200 °C offers a bright cyan coloration.

References

[1] J. Merikhi, H.-O. Jungk, C. Feldmann, Sub-micrometer $CoAl_2O_4$ pigment particles - synthesis and preparation of coatings, J. Mater. Chem. 10 (2000) 1311–1314.

[2] K. Hudson, H. Winbow, J. Cowley, Colors for ceramic bodies, Ceram. Eng. Sci. Proc. 17 (1996) 102–110.

[3] M.I.B. Bernardi, C.A.C. Feitosa, C.A. Paskocimas, E. Longo, C.O. Paiva-Santos, Development of metal oxide nanoparticles by soft chemical method, Ceram. Int. 35 (2009) 463–466.

[4] T. Suzuki, H. Nagai, M. Nohara, H. Takagi, Melting of antiferromagnetic ordering in spinel oxide $CoAl_2O_4$, J. Phys. Condens. Mat. 19 (2007) 14265.

[5] F. Tielens, M. Calatayud, R. Franco, J.M. Recio, M. Pérez-Ramírez, C. Minot, Periodic DFT study of the structural and electronic properties of bulk $CoAl_2O_4$ spinel, J. Phys. Chem. B 110 (2006) 988–995.

[6] C. Angeletti, F. Pepe, P. Porta, Structure and catalytic activity of $Co_xMg_{1-x}Al_2O_4$ spinel solid solutions, Part 1. Distribution of Co^{2+} ions Cation, J. Chem. Soc. 73 (1977) 1972–1982.

[7] M. Zayat, D. Levy, Blue $CoAl_2O_4$ particles prepared by the sol–gel and citrate-gel methods, Chem. Mater. 12 (2000) 2763–2769.

[8] P. Garcia Casado, I. Rasines, The series of spinels $Co_{3-s}Al_sO_4$ ($0 < s < 2$): study of Co_2AlO_4, J. Solid State Chem. 52 (1984) 187–190.

[9] G. Monari, T. Mandefrini, Coloring effects of synthetic inorganic cobalt pigments in fast-fired porcelainized tiles, Ceram. Eng. Sci. Proc. 17 (1996) 167–172.

[10] M. Llusar, A. Forès, J.A. Badenes, J. Calbo, M.A. Tna, G. Monros, Color analysis of some cobalt-based blue pigments, J. Eur. Ceram. Soc. 21 (2001) 1121–1130.

[11] R. Pozas, V.M. Orera, M. Ocana, Hydrothermal synthesis of Co-doped willemite powders with controlled particle size and shape, J. Eur. Ceram. Soc. 25 (2004) 3165–3172.

[12] W. Li, J. Li, J. Guo, Synthesis and characterization of nanocrystalline $CoAl_2O_4$ spinel powder by low temperature combustion, J. Eur. Ceram. Soc. 23 (2003) 2289–2295.

[13] D.M.A. Melo, J.D. Cunha, J.D.G. Fernandes, M.I. Bernardi, M.A.F. Melo, A.E. Martinelli, Evaluation of $CoAl_2O_4$ as ceramic pigments, Mat. Res. Bull. 38 (2003) 1559–1564.

[14] X. Duan, D. Yuan, Z. Sun, C. Luan, D. Pan, D. Xu, M. Lv, Preparation of Co^{2+}-doped $ZnAl_2O_4$ nanoparticles by citrate sol-gel method, J. Alloy Compd. 386 (2005) 311–314.

[15] W.-S. Cho, M. Kakihana, Crystallization of ceramic pigment $CoAl_2O_4$ nanocrystals from Co–Al metal organic precursor, J. Alloy Compd. 287 (1999) 87–90.

[16] M. Gaudon, A. Apheceixbordes, M. Ménétrier, A. Le Nestour, A. Demourgues, Synthesis temperature effect on the structural features and optical absorption of $Zn_{1-x}Co_xAl_2O_4$ oxides, Inorg. Chem. 48 (2009) 9085 (91).

[17] I.S. Ahmed, H.A. Dessouki, A.A. Ali, Synthesis and characterization of $Ni_xMg_{1-x}Al_2O_4$ nano ceramic pigments via a combustion route, Polyhedron 30 (2011) 584–591.

[18] D. Visinescu, F. Papa, A.C. Ianculescu, I. Balint, O. Carp, Nickel-doped zinc aluminate oxides: Starch-assisted synthesis, structural, optical properties, and their catalytic activity in oxidative coupling of methane, J. Nanopart. Res. 15 (2013) 1456.

[19] G. Lorenzi, G. Baldi, F. Di Benedetto, V. Faso, P. Lattanzi, M. Romanelli, Spectroscopic study of a Ni-bearing gahnite pigment, J. Eur. Ceram. Soc. 26 (2006) 317–321.

[20] D. Visinescu, C. Paraschiv, A. Ianculescu, B. Jurca, B. Vasile, O. Carp, The environmentally benign synthesis of nanosized $Co_xZn_{1-x}Al_2O_4$ blue pigments, Dyes Pigm. 87 (2010) 125–131.

[21] A. Fernàndez-Osorio, E. Pineda-Villanueva, J. Chàvez-Fernàndez, Synthesis of nanosized $(Zn_{1-x}Co_x)Al_2O_4$ spinels: new pink ceramic pigments, Mater. Res. Bul. 47 (2012) 445–452.

[22] H.S.C. O'Neill, Temperature dependence of the cation distribution in $CoAl_2O_4$ spinel, Eur. J. Mineral. 6 (1994) 603.

[23] J. Popovic, E. Tkalčec, B. Gržeta, S. Klrajica, B. Rakvin, Inverse spinel structure of co-doped gahnite, Am. Mineral. 94 (2009) 771–776.

[24] L.K.C. de Souza, J.R. Zamian, G.N. da Rocha Filho, L.E.B. Soledade, I.M.G. dos Santos, A.G. Souza, T. Scheller, R.S. Angélica, C.E.F. da Costa, Blue pigments based on $Co_xZn_{1-x}Al_2O_4$ spinels synthesized by the polymeric precursor method, Dyes Pigm. 81 (2009) 187–192.

[25] N. Pechini, Method of Preparing Lead and Alkaline Earth Titanates and Niobates and Coating Method Using the Same to Form, Patent No. 3,330, 697 1967.

[26] P.h. Tailhades, C. Villette, A. Rousset, G.U. Kulkarni, K.R. Kannan, C.N.R. Rao, M. Lenglet, Cation migration and coercivity in mixed copper–cobalt spinel ferrite powders, J. Solid State Chem. 141 (1998) 56–63.

[27] J. Rodriguez-Carvajal. FULLPROF: a program for Rietveld refinement and pattern matching analysis. Abstracts of the Satellite Meeting on Powder Diffraction of the XV Congress of the IUCr, Toulouse, France; 1990, p. 127.

[28] V. Sepelak, I. Bergmann, S. Indris, A. Feldhoff, H. Hahn, K.D. Becker, C.P. Gray, P. Heitjans, High-resolution ^{27}Al MAS NMR spectroscopic studies of the response of spinel aluminates to mechanical action J. Mater. Chem. 21 (2011) 8332–8337.

[29] N. Pellerin, C. Dodane-Thiriet, V. Montouillout, M. Beauvy, D. Massiot, Cation sublattice disorder induced by swift heavy ions in $MgAl_2O_4$ and $ZnAl_2O_4$ spinels: ^{27}Al solid-state NMR study, J. Phys. Chem. B 111 (2007) 12707–12714.

[30] V. Sreeja, T.S. Smitha, D. Nand, T.G. Ajithkumar, P.A. Joy, Size dependent coordination behavior and cation distribution in $MgAl_2O_4$ nanoparticles from ^{27}Al solid state NMR studies, J. Phys. Chem. C 112 (2008) 14737–14744.

[31] V. Sepelak, S. Indris, I. Bergmann, A. Feldhoff, K.D. Becker, P. Heitjans, Nonequilibrium cation distribution in nanocrystalline $MgAl_2O_4$ spinel studied by ^{27}Al magic-angle spinning NMR, Solid State Ionics 177 (2006) 2487–2490.

[32] P. Jeevanandam, Yu. Koltypin, A. Gedanken, Preparation of nanosized nickel aluminate spinel by a sonochemical method, Mater. Sci. Eng. B 90 (2002) 125–132.

[33] C.F. Song, M.K. Lu, F. Gu, S.W. Liu, S.F. Wang, D. Xu, D.R. Yuan, Effect of Al^{3+} on the photoluminescence properties of Ni^{2+}-doped sol-gel SiO^2 glass, Inorg. Chem. Commun. 6 (2003) 523–526.

[34] T. Bates, Ligand field theory and absorption spectra of transition-metal ions in glasses, in: D. Mackenzie (Ed.), Modern Aspects of the Vitreous State, vol. 2, Butterworths Inc., London, 1961, pp. 195–254.